

# Power-Optimal HARQ Protocol for Reliable Free Space Optical Communication

Georgios D. Chondrogiannis\*, Nikos A. Mitsiou\*, Nestor D. Chatzidiamantis\*,  
Alexandros-Apostolos A. Boulogeorgos<sup>†</sup>, and George K. Karagiannidis\*<sup>‡</sup>

\*Department of Electrical and Computer Engineering, Aristotle University of Thessaloniki, GR-54124 Thessaloniki, Greece  
Emails: {gchondro,nmitsiou,nestoras,geokarag}@auth.gr

<sup>†</sup>Department of Electrical and Computer Engineering, University of Western Macedonia, 50100 Kozani, Greece.  
Emails: al.boulogeorgos@ieee.org

<sup>‡</sup>Cyber Security Systems and Applied AI Research Center, Lebanese American University (LAU), Lebanon

**Abstract**—This paper investigates the usage of hybrid automatic repeat request (HARQ) protocols for power-efficient and reliable communications over free space optical (FSO) links. By exploiting the large coherence time of the FSO channel, the proposed transmission schemes combat turbulence-induced fading by retransmitting the failed packets in the same coherence interval. To assess the performance of the presented HARQ technique, we extract a theoretical framework for the outage performance. In more detail, a closed-form expression for the outage probability (OP) is reported and an approximation for the high signal-to-noise ratio (SNR) region is extracted. Building upon the theoretical framework, we formulate a transmission power allocation problem throughout the retransmission rounds. This optimization problem is solved numerically through the use of an iterative algorithm. In addition, the average throughput of the HARQ schemes under consideration is examined. Simulation results validate the theoretical analysis under different turbulence conditions and demonstrate the performance improvement, in terms of both OP and throughput, of the proposed HARQ schemes compared to fixed transmit power HARQ benchmarks.

## I. INTRODUCTION

Free space optical (FSO) communication has emerged as a promising technology that can compensate for the growing scarcity of the radio-frequency spectrum. High-speed, wide bandwidth and low-cost wireless data transfer are some of the key benefits that FSO brings, despite the fact that the reliability of those systems has been a problem especially for long distances and foggy atmospheric conditions [1]. As an enabler for ensuring an all-weather reliable FSO link over transmission distances of few kilometers, error-control retransmission protocols, that take into consideration the interconnection between the physical and the link layer, has been identified.

A recently proposed scheme for error-control retransmissions is the combination of automatic repeat request (ARQ) and forward error correction (FEC), the so-called hybrid ARQ (HARQ). Specifically, ARQ realizes the transmission of erroneously received packets based on the feedback from the receiver, while FEC accomplishes the correction of received data errors by adding a few redundant bits to the transmitted data. Thus, transmission reliability is improved, which simultaneously boosts the system's throughput [2].

Several HARQ retransmission schemes have been proposed in the context of FSO communications (e.g. [3] and the references therein). Among them, two types have attracted par-

ticular interest, namely, HARQ with code combining (HARQ-CC) and HARQ with incremental redundancy (HARQ-IR). In both, previously failed packets are stored and combined with subsequent retransmissions for decoding. Specifically, in HARQ-CC the same packet is retransmitted, while in HARQ-IR redundant information is incrementally transmitted in each round. HARQ-CC and HARQ-IR schemes were investigated in [4], where an outage analysis under turbulence induced fading was documented. A similar analysis was presented in [5], [6], where pointing and misalignment errors were also taken into account. Moreover, other performance metrics such as waiting and sojourn times, were investigated in [7]. Note that in all existing HARQ retransmission protocols, any constraints regarding the power consumption that may exist at the FSO transmitter are not considered. Furthermore, it is assumed that each transmission attempt uses equal transmit power.

However, the assumption of unlimited power consumption at the transmitter is not always valid. For example, energy restriction issues may arise when FSO links are established between a fixed-point station and moving entities, such as unmanned aerial vehicles, High-altitude platform stations (HAPS) or satellites [8]. In the view of the above, we present two energy efficient HARQ retransmission protocols that modify the parameters in each transmission round such that the outage probability (OP) is minimized, while reducing the power-consumption at the transmitter's side as well. In particular, the contribution of the paper is summarized below:

- We investigate the performance of HARQ-CC and HARQ-IR protocols, under the assumption that the use of interleaving is impractical in FSO links due to their large coherence times [9]. Closed-form, analytical expressions are derived for the OP of each protocol, while taking into account both atmospheric and misalignment effects.
- We further elaborate on the case of high signal-to-noise ratio (SNR) regime and derive tractable and insightful expressions for the outage performance of both protocols.
- Based on the high SNR OP analysis, we address the problem of minimizing the OP and the average throughput subject to average and peak optical power constraints. Due to its non-convexity, a tractable solution is proposed, via the concept of successive convex approximation (SCA).

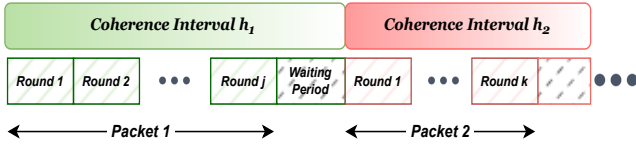


Fig. 1: Relation between coherence intervals and packet transmission duration.

- Simulation results validate the theoretical analysis for the OP of both HARQ-CC and HARQ-IR. Also, optimized HARQ-CC and optimized HARQ-IR are shown to outperform their respective fixed power HARQ benchmarks, both in terms of OP and throughput.

## II. SYSTEM MODEL

We consider a point-to-point intensity modulation-direct detection (IM/DD) FSO system where HARQ transmission schemes are employed. The received signal in the  $i$ -th transmission round can be expressed as

$$\mathbf{y}_i = \mathcal{R}P_i h_i \mathbf{x}_i + \mathbf{n}_i, \text{ with } i = 1, 2, \dots, J \quad (1)$$

where  $\mathbf{x}_i$  is the  $i$ -th modulated optical signal with unitary mean, i.e.  $\mathbb{E}[\mathbf{x}_i] = 1$ ,  $h_i$  stands for the  $i$ -th channel coefficient that models the fading process and  $\mathbf{n}_i$  represents the zero-mean Gaussian noise at the receiver site at the  $i$ -th transmission round with variance  $\sigma_n^2$ , i.e.,  $\mathbf{n}_i \sim N(0, \sigma_n^2)$ . Furthermore,  $\mathcal{R}$  is the receiver's responsivity and  $P_i$  is the optical transmit power that satisfies  $P_i \leq P_{max}$  imposed by safety and physical limitations.

It should be noted that the optical channel results in a very slowly-varying fading in FSO systems. For the signalling rates of interest ranging from hundreds to thousands of Mbps [10], turbulence-induced fading can be considered constant over hundred of thousand or millions of consecutive symbols, since the coherence time of the channel is about 1-100 ms [1]. This fact leads to consider interleaving an unviable solution for averaging a large number of fading states, since the demands in storage memory would be unrealistic. In the proposed transmission model, as depicted in Fig. 1, each packet consists of several transmission rounds (at most  $J$ ) and multiple transmitted symbols. Every packet experiences a different fading realization, where the independence between them is ensured through an idle waiting period.

In the analysis that follows, it is assumed that the transmitter has statistical knowledge of the channel gains, i.e., statistical channel state information (CSI). This assumption is practical as it does not require extensive feedback from the receiver and suffices to know only the statistical parameters of the fading distribution (e.g. the probability density function of the SNR).

### A. Channel model

The channel fading state,  $h$ , is considered to be the product of three factors, i.e.,  $h = h_l h_s h_g$ . The first term,  $h_l$ , denotes the deterministic path loss exponent, which depends from link distance and weather conditions. The second term,  $h_g$ , corresponds to the misalignment loss between the transmitter

(TX) and the receiver (RX), i.e., pointing errors, of the optical point-to-point channel. Assuming a Gaussian beam profile at the receiver, the attenuation due to geometric spread with radial displacement from the origin of the detector follows a Rayleigh distribution. Finally, the third term stands for the attenuation due to the atmospheric turbulence conditions, i.e., scintillation [9]. We consider the widely used Gamma-Gamma atmospheric attenuation model, in order to include a wide range of weak to strong turbulence conditions [1].

By combining the above statistical models, the probability density function (PDF) of  $h = h_l h_s h_g$  is given as [11]

$$f_h(h) = \frac{\alpha\beta\xi^2}{A_0 h_l \Gamma(\alpha)\Gamma(\beta)} \times G_{1,3}^{3,0} \left[ \alpha\beta \frac{h}{A_0 h_l} \mid \xi^2 - 1, \alpha - 1, \beta - 1 \right], \quad (2)$$

where  $\alpha$  and  $\beta$  are the statistical parameters that define the atmospheric turbulence conditions of the optical link [1]. Furthermore,  $\xi$  is the ratio between the equivalent beam radius at the receiver and the pointing error misplacement standard deviation at the receiver site ( $\xi \rightarrow \infty$  corresponds to the case where there's no pointing errors).  $A_0$  denotes a constant term of the pointing loss which represents the power collected at the detector's center. Finally,  $G_{p,q}^{m,n}[\cdot]$  is the Meijer's G-function [12, Eq. (9.301)]

### B. Instantaneous SNR Statistics

From (1), the instantaneous electrical SNR of the received signal in the  $i^{\text{th}}$  transmission round is defined as

$$\gamma_i = \frac{\mathcal{R}^2 P_i^2 h_i^2}{\sigma_n^2}. \quad (3)$$

Based on (3), the cumulative distribution function (CDF) of the instantaneous SNR are derived as [13]

$$F_{\gamma_i}(\gamma_i) = \frac{\xi^2}{\Gamma(\alpha)\Gamma(\beta)} G_{2,4}^{3,1} \left[ \frac{\alpha\beta}{P_i} \sqrt{\frac{\gamma_i}{\bar{\gamma}}} \mid 1, \xi^2 + 1 \right], \quad (4)$$

respectively, where

$$\bar{\gamma} = \frac{A_0^2 h_l^2 \xi^2}{\sigma_n^2 (\xi^2 + 1)} \stackrel{\xi^2 \gg 1}{\approx} \frac{A_0^2 h_l^2}{\sigma_n^2} \quad (5)$$

is the average received electrical SNR. Without loss of generality the receiver's responsivity is assumed to be unitary. Also the fading coefficient is given by  $h_i = (A_0 h_l / P_i) \sqrt{\gamma_i / \bar{\gamma}}$ .

## III. HARQ TRANSMISSION PROTOCOLS

In this section, we investigate the performance of H-ARQ transmission protocols that can be applied in FSO systems and present optimal power allocation design strategies among transmission rounds. It is assumed that one-bit messages of positive or negative acknowledgement (ACK or NACK, respectively) are exchanged between TX and RX through a reliable and a zero-delay feedback channel.

### A. Code Combining HARQ

In HARQ-CC, the TX sends the same codeword until an ACK is received or the maximum number of retransmissions  $J$  is reached. At the RX's end, all the received copies of the encoded packet are combined using maximal ratio combining (MRC) and then the decoding method (e.g. Maximum likelihood) is performed. If the decoding attempt is successful an ACK message is sent back to the TX.

By the end of the  $j$ -th transmission round, the accumulated mutual information is equal with [14], [15]

$$I_j^{\text{CC}} = \frac{1}{2j} \log_2 \left( 1 + c \sum_{i=1}^j \gamma_i \right), \quad (6)$$

where  $c = \frac{1}{2\pi e}$  in IM/DD, if both peak-power and average-power constraints are imposed on the transmitted signal. By defining OP in  $j$ -th transmission round as the probability of the accumulated mutual information being smaller than the transmission rate  $R$ , it follows that

$$\begin{aligned} \mathbb{P}_{\text{out},j}^{\text{CC}}(\mathbf{P}, R) &= \Pr \left\{ I_j^{\text{CC}} \leq \frac{R}{j} \right\} \\ &= \Pr \left\{ h^2 \leq \frac{A_0^2 h_l^2 (2^{2R} - 1)}{c\gamma \sum_{i=1}^j P_i^2} \right\}, \end{aligned} \quad (7)$$

where  $\mathbf{P} = (P_1, \dots, P_j)$  is the vector of the transmitted power across  $j$  HARQ rounds. After using (4) and some basic algebraic manipulations, OP is calculated by

$$\begin{aligned} \mathbb{P}_{\text{out},j}^{\text{CC}}(\mathbf{P}, R) &= \frac{\xi^2}{\Gamma(\alpha)\Gamma(\beta)} \\ &\times G_{2,4}^{3,1} \left[ \alpha\beta \sqrt{\frac{2^{2R} - 1}{c\gamma \sum_{i=1}^j P_i^2}} \mid 1, \xi^2 + 1 \right]. \end{aligned} \quad (8)$$

1) *High-SNR analysis:* In order to gain insights about the behavior of the proposed system the asymptotic analysis for the two protocols is performed.

**Theorem 1.** *In high-SNR region, the OP is approximated as*

$$\mathbb{P}_{\text{out},j}^{\text{CC}} \stackrel{\gamma_i \gg 1}{\cong} \begin{cases} \frac{\Gamma(\alpha - \xi^2)\Gamma(\beta - \xi^2)}{\Gamma(\alpha)\Gamma(\beta)} \left( \frac{V_R}{\sum_{i=1}^j P_i^2} \right)^{\xi^2/2}, & \xi^2 < q(\alpha, \beta) \\ C(\alpha, \beta) \left( \frac{V_R}{\sum_{i=1}^j P_i^2} \right)^{q(\alpha, \beta)/2}, & \xi^2 > q(\alpha, \beta) \end{cases} \quad (9)$$

where  $q(\alpha, \beta) = \min\{\alpha, \beta\}$ ,  $V_R = \alpha^2 \beta^2 (2^{2R} - 1) / c\gamma$  and  $C(\alpha, \beta) = \frac{\Gamma(|\beta - \alpha|)}{(1 - q(\alpha, \beta) / \xi^2) \Gamma(q(\alpha, \beta) + 1) \Gamma(\alpha\beta / q(\alpha, \beta))}$ .

*Proof:* The proof is provided in Appendix A. ■

By defining

$$\psi_R(\alpha, \beta) = \begin{cases} \frac{\Gamma(\alpha - \xi^2)\Gamma(\beta - \xi^2)}{\Gamma(\alpha)\Gamma(\beta)} V_R^{\xi^2/2} & \text{for } \xi^2 < q(\alpha, \beta) \\ C(\alpha, \beta) V_R^{q(\alpha, \beta)/2} & \text{for } \xi^2 > q(\alpha, \beta) \end{cases} \quad (10)$$

becomes evident that the asymptotic OP can be written as

$$\mathbb{P}_{\text{out},j}^{\text{CC}} \approx \frac{\psi_R(\alpha, \beta)}{\left( \sum_{i=1}^j P_i^2 \right)^{\frac{\min(\xi^2, \alpha, \beta)}{2}}}. \quad (11)$$

The average power across all rounds can be written as [16]

$$\bar{P} = P_1 + \sum_{j=2}^J P_j \mathbb{P}_{\text{out},j-1}^{\text{CC}}. \quad (12)$$

2) *HARQ-CC Optimization:* The problem addressed in this section is the optimal power allocation across the HARQ-CC rounds in order to minimize the OP subject to an average power constraint. To make the following optimization problem tractable we adopt the high-SNR analysis for the optical link. Thus, the optimization problem can be formulated as follows:

$$\begin{aligned} \min_{P_1, P_2, \dots, P_J} \quad & \mathbb{P}_{\text{out},J}^{\text{CC}} \\ \text{s.t.} \quad & P_1 + \sum_{j=2}^J \frac{P_j \psi_R(\alpha, \beta)}{\left( \sum_{i=1}^{j-1} P_i^2 \right)^{\frac{\min(\xi^2, \alpha, \beta)}{2}}} \leq P_0, \\ & 0 \leq P_j \leq P_{\max}, \quad \forall j \in \{1, \dots, J\}, \end{aligned} \quad (13)$$

where  $P_0$  expresses the average power constraint and  $P_{\max}$  denotes a peak power limitation for every round  $j \in \{1, \dots, J\}$ . Note that the formulated problem is non-convex, due to both the imposed non-convex average power constraint and the objective function. As such, a viable solution cannot be provided. To that end, the following auxiliary variables  $t_j$ ,  $\forall j \in \{2, \dots, J\}$ , are introduced for which it holds

$$\frac{P_j \psi_R(\alpha, \beta)}{\left( \sum_{i=1}^{j-1} P_i^2 \right)^{\frac{\min(\xi^2, \alpha, \beta)}{2}}} \leq t_j. \quad (14)$$

Also, the auxiliary variables  $\tilde{P}_j$  will be used, so that  $\tilde{P}_j = P_j^2, \forall j \in \{1, \dots, J\}$ . By using the properties of the natural logarithm, the optimization problem can be rewritten as

$$\begin{aligned} \min_{P_1, P_2, \dots, P_J} \quad & - \frac{\min(\xi^2, \alpha, \beta)}{2} \log \left( \sum_{j=1}^J \tilde{P}_j \right) \\ \text{s.t.} \quad & \sqrt{\tilde{P}_1} + \sum_{j=2}^J t_j \leq P_0 \\ & \log(\psi_R(a, b)) + \frac{1}{2} \log(\tilde{P}_j) - \log(t_j) \\ & - \frac{\min(\xi^2, \alpha, \beta)}{2} \log \left( \sum_{i=1}^{j-1} \tilde{P}_i \right) \leq 0, \\ & \forall j \in \{2, \dots, J\} \\ & 0 \leq \tilde{P}_j \leq P_{\max}^2, \forall j \in \{1, \dots, J\}. \end{aligned} \quad (15)$$

The problem is still non-convex, due to the concave terms  $\sqrt{\tilde{P}_1}$  and  $\log(\tilde{P}_j)$  in the constraints. To overcome this, the concept of SCA is utilized. The first order Taylor expansion

of the concave terms, around the randomly chosen initial point  $\tilde{P}_{j,0}$ , is given by

$$\sqrt{\tilde{P}_1} \approx \sqrt{\tilde{P}_{1,0}} + \frac{1}{2} \tilde{P}_{1,0}^{-\frac{1}{2}} (\tilde{P}_1 - \tilde{P}_{1,0}), \quad (16)$$

$$\log(\tilde{P}_j) \approx \log(\tilde{P}_{j,0}) + \frac{\tilde{P}_j - \tilde{P}_{j,0}}{\tilde{P}_{j,0}}. \quad (17)$$

By substituting in (15), the problem which arises is convex. Thus, it can be solved by standard convex optimization methods, such as the interior-point method. Moreover, due to the SCA, the solution of (15) requires to solve its convex version multiple times, which is shown in Algorithm 1.

---

#### Algorithm 1 HARQ-CC optimization

---

- 1: initialize FSO parameters,  $\tilde{\mathbf{P}}_0$ ,  $\delta_{\max}$  and  $\epsilon$
  - 2: **while**  $\delta < \delta_{\max}$  AND  $\|\tilde{\mathbf{P}}_\delta^* - \tilde{\mathbf{P}}_{\delta-1}^*\|_2^2 > \epsilon$  **do**
  - 3:      $\delta \leftarrow \delta + 1$
  - 4:     Solve the convex version of (15), obtain  $\tilde{\mathbf{P}}_\delta^*$
  - 5:      $\tilde{\mathbf{P}}_0 \leftarrow \tilde{\mathbf{P}}_\delta^*$
  - 6: **end while**
  - 7:  $\mathbf{P}^* \leftarrow \tilde{\mathbf{P}}_\delta^*$
- 

#### B. Incremental Redundancy H-ARQ

In incremental redundancy protocol the source of the TX encodes the information message with a punctured version of a (low-rate) mother FEC code. At the initial transmission, only a few parity bits of the original code are transmitted along with the information message. If a decoding failure occurs, in the following rounds, the TX keeps sending additional redundant bits according to the puncturing pattern of the mother code. At the other side, the RX combines the parity bits of the previous rounds with the most recently received ones and performs joint decoding. This particular scheme induces some extra complexity to the operation of both the TX and the RX, which comes as a consequence of the composite decoding process.

1) *Performance Analysis:* The transmission rate for the first round,  $R$ , becomes  $R/j$  after the passage of  $j$  rounds and the accumulated mutual information can be obtained as

$$I_j^{\text{IR}} = \frac{1}{2j} \sum_{i=1}^j \log_2(1 + c\gamma_i), \quad (18)$$

and the OP is defined as

$$\mathbb{P}_{\text{out},j}^{\text{IR}}(\mathbf{P}, R) = \Pr \left\{ I_j^{\text{IR}} \leq \frac{R}{j} \right\}. \quad (19)$$

We obtain an expression for the OP with the following approximation [17].

$$\begin{aligned} \mathbb{P}_{\text{out},j}^{\text{IR}} &\simeq \Pr \left\{ \log_2 \left( 1 + \left( c\bar{\gamma} \frac{h^2}{A_0^2 h_l^2} \right)^j \prod_{i=1}^j P_i^2 \right) \leq 2R \right\} \\ &= \Pr \left\{ h^2 \leq \frac{A_0^2 h_l^2}{c\bar{\gamma}} \left( \frac{2^{2R} - 1}{\prod_{i=1}^j P_i^2} \right)^{1/j} \right\} \end{aligned} \quad (20)$$

Similar with (7), the OP is given by

$$\begin{aligned} \mathbb{P}_{\text{out},j}^{\text{IR}}(\mathbf{P}, R) &= \frac{\xi^2}{\Gamma(\alpha)\Gamma(\beta)} \\ &\times G_{2,4}^{3,1} \left[ \frac{\alpha\beta}{\sqrt{c\bar{\gamma}}} \left( \frac{2^{2R} - 1}{\prod_{i=1}^j P_i^2} \right)^{1/2j} \mid \begin{matrix} 1, \xi^2 + 1 \\ \xi^2, \alpha, \beta, 0 \end{matrix} \right] \end{aligned} \quad (21)$$

2) *High-SNR analysis:* Following the same methodology as in Section III, the OP can be asymptotically derived as:

$$\mathbb{P}_{\text{out},j}^{\text{CC}} \approx \frac{\theta_{R,j}(\alpha, \beta)}{\left( \prod_{i=1}^j P_i \right)^{\frac{\min(\xi^2, \alpha, \beta)}{j}}} \quad (22)$$

where the nominator is given by

$$\theta_{R,j}(\alpha, \beta) = \begin{cases} \frac{\Gamma(\alpha - \xi^2)\Gamma(\beta - \xi^2)}{\Gamma(\alpha)\Gamma(\beta)} U_{R,j}^{\xi^2/2j} & \text{for } \xi^2 < q(\alpha, \beta) \\ C(\alpha, \beta) U_{R,j}^{q(\alpha, \beta)/2j} & \text{for } \xi^2 > q(\alpha, \beta) \end{cases} \quad (23)$$

$$\text{and } U_{R,j} = \left( \frac{\alpha^2 \beta^2}{c\bar{\gamma}} \right)^j (2^{2R} - 1)$$

3) *HARQ-IR Optimization:* In this section, the optimal power allocation across the HARQ-IR rounds is addressed. By applying a similar approach as in Section III, the optimization problem that arises is formulated as:

$$\begin{aligned} \min_{P_1, P_2, \dots, P_J} \quad & \mathbb{P}_{\text{out},J}^{\text{IR}} \\ \text{s.t.} \quad & P_1 + \sum_{j=2}^J \frac{P_j \theta_{R,j}(\alpha, \beta)}{\left( \prod_{i=1}^{j-1} P_i \right)^{\frac{\min(\xi^2, \alpha, \beta)}{j}}} \leq P_0 \\ & 0 \leq P_j \leq P_{\max}, \quad \forall j \in \{1, \dots, J\} \end{aligned} \quad (24)$$

The problem of (24) is nonconvex. However, it can be proven that (24) can be formulated as convex. Due to space limitation the analytic transformation is not given, nonetheless, by following a similar approach as in the HARQ-CC scheme (24) is transformed into a convex form.

#### C. Average Throughput

In order to gain a general perspective on the impact of power allocation to the FSO system, we investigate the throughput of the system throughout the implementation of the above techniques. The average throughput of HARQ schemes is defined as the average number of successfully delivered bits per channel use (bps/channel use) [2]. We are interested in finding the optimal power allocation  $\mathbf{P}^*$  and the optimal value of the transmission rate  $R$ , for which the throughput is maximized. This can be described by the following optimization problem:

$$\begin{aligned} \max_{\mathbf{P}^*, R} \quad & \omega_J = \frac{R(1 - \mathbb{P}_{\text{out},J})}{1 + \sum_{j=1}^{J-1} \mathbb{P}_{\text{out},j}} \\ \text{s.t.} \quad & P_1 + \sum_{j=2}^J P_j \mathbb{P}_{\text{out},j-1} \leq P_0 \\ & 0 \leq P_j \leq P_{\max}, \quad \forall j \in \{1, \dots, J\}, \end{aligned} \quad (25)$$

where  $\mathbb{P}_{\text{out},j}$  refers to either HARQ-CC or HARQ-IR protocol and the constraints are imposed from the assumed average and maximum optical power constraints of the FSO system. The problem is non-convex, however, it can be efficiently solved by utilizing the analysis of Section III, since, for a fixed value of  $R$ , maximizing the objective value of (25) is equivalent to maximizing  $(1 - \mathbb{P}_{\text{out},J})$ . The intuitive reason for that is that  $(1 - \mathbb{P}_{\text{out},J})$  describes the probability of having a successful transmission at any round  $j \in \{1, \dots, J\}$ . Thus, maximizing that probability, also minimizes the OP of  $\mathbb{P}_{\text{out},j}, \forall j \in \{1, \dots, J\}$ . Hence, by performing a linear search on  $R$ , problem (25) can be solved by finding the optimal solution of (14) for the HARQ-CC case, or (26) for the HARQ-IR case.

Parameters	Symbol	Value
Average power constraint	$P_0$	200 mW
Maximum available power	$P_{\text{max}}$	350 mW
Maximum retransmissions	$J$	4
Link range	$l$	1 km
Receiver radius	$r$	10 cm
Attenuation coefficient	$d_a$	$\simeq 0.1$
Ratio of EBR and the jitter	$\xi$	4
Noise standard deviation	$\sigma_n$	$10^{-7}$ A
Jitter standard deviation	$\sigma_s$	30 cm
Algorithm 1 convergence threshold	$\epsilon$	$10^{-5}$
Algorithm 1 iterations allowed	$\delta_{\text{max}}$	50

#### IV. RESULTS AND DISCUSSION

In this section, simulations are presented to validate the presented performance analysis and also to demonstrate the effectiveness of the presented power allocation optimization problems. Unless otherwise stated, the simulation parameters are given in Table I. For the case of moderate turbulence we assumed  $\alpha = 2.296$ ,  $\beta = 1.822$ , while for the case of strong turbulence we considered  $\alpha = 2.064$ ,  $\beta = 1.342$ .

In Fig. 2, simulation and theoretical results are displayed for moderate and strong turbulence conditions when equal power allocation is performed across different HARQ rounds. It becomes obvious from the figure that analytical results coincide with simulations for the HARQ-CC scheme; thus validating theoretical analysis. On the other hand, regarding HARQ-IR scheme, there is a slight error between simulation and analytical results which was emerged from the approximation of OP. It's visible that the approximate expression forms a tight upper-bound across the whole range of considered SNR values. In addition, it can be observed that HARQ-IR performs better from HARQ-CC in terms of OP for different fading conditions. Finally, as a benchmark, analytical results for the cases of  $J = 1$  (without HARQ) and  $J = 10$  are also included in the same figure, revealing the effectiveness of HARQ schemes as the number of retransmissions increases as well as the fast convergence to the extreme case.

In Fig. 3, the OP is plotted against different values of the target rate  $R$  for moderate turbulent conditions. As benchmarks, the HARQ-CC and the HARQ-IR schemes with constant power during each round  $j, \forall j \in \{1, \dots, J\}$ , namely  $P_j = P_0/J$ , are also depicted in the figure. It can be seen that by

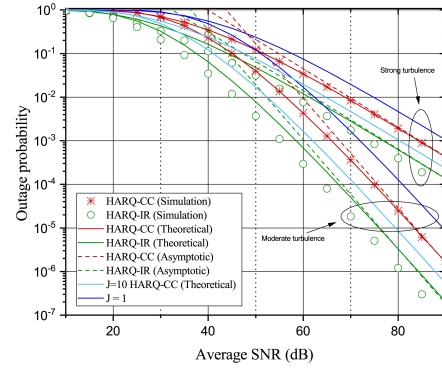


Fig. 2: OP for different turbulent conditions,  $R = 2$  bits/s/Hz,  $P = P_{\text{max}}$

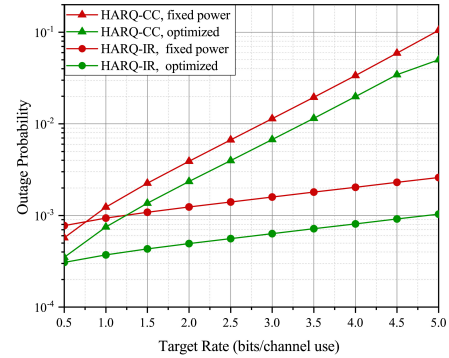


Fig. 3: OP vs the target rate,  $\bar{\gamma} = 60$ dB.

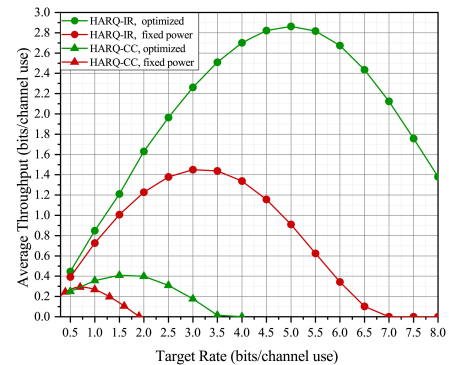


Fig. 4: Average Throughput vs the target rate,  $\bar{\gamma} = 30$ dB.

proper power allocation, as presented in section III, significant improvement in terms of OP is achieved. Specifically, the optimized HARQ-CC outage performance is three times better compared to its non-optimized version, while the optimized HARQ-IR is about five times better than its non-optimized counterpart. For low  $R$ , retransmissions are barely exploited; therefore, the performance of both protocols is similar. However, HARQ-IR completely dominates the HARQ-CC protocol for greater values of rates  $R$ , due to increased complexity.

In Fig. 4, the optimized average throughput, as given in section III, is illustrated for moderate turbulence. For the HARQ-CC protocol, it is observed that its optimized version offers a peak average throughput of 0.4 bits/channel while its non-optimized counterpart achieves 0.3 bits/channel peak

$$\begin{aligned}
\mathbb{P}_{\text{out},j}^{\text{CC}} &= \frac{\Gamma(\alpha - \xi^2) \Gamma(\beta - \xi^2)}{\Gamma(\alpha) \Gamma(\beta)} \left( \frac{V_R}{\sum_{i=1}^j P_i^2} \right)^{\xi^2/2} + \frac{\Gamma(\beta - \alpha)}{(1 - \alpha/\xi^2) \Gamma(\alpha + 1) \Gamma(\beta)} \left( \frac{V_R}{\sum_{i=1}^j P_i^2} \right)^{\alpha/2} \\
&\times {}_2F_3 \left( \alpha, \alpha - \xi^2; 1 + \alpha - \xi^2, 1 + \alpha - \beta, 1 + \alpha; \sqrt{\frac{V_R}{\sum_{i=1}^j P_i^2}} \right) + \frac{\Gamma(\alpha - \beta)}{(1 - \beta/\xi^2) \Gamma(\beta + 1) \Gamma(\alpha)} \left( \frac{V_R}{\sum_{i=1}^j P_i^2} \right)^{\beta/2} \\
&\times {}_2F_3 \left( \beta, \beta - \xi^2; 1 + \beta - \xi^2, 1 + \beta - \alpha, 1 + \beta; \sqrt{\frac{V_R}{\sum_{i=1}^j P_i^2}} \right), \text{ with } V_R = \alpha^2 \beta^2 (2^{2R} - 1) / c\bar{\gamma}
\end{aligned} \tag{26}$$

average throughput. Furthermore, the optimized HARQ-IR is shown to be doubled compared to the fixed power HARQ-IR benchmark. In particular, the optimized power HARQ-IR scheme achieves 2.8 bits/channel use, while its fixed power counterpart achieves 1.4 bits/channel use. Thus, it is evident that the power allocation in HARQ schemes greatly improve the efficiency of the FSO system.

## V. CONCLUSIONS

In this paper we explored the power efficient and reliable employment of the HARQ protocol for FSO communications. In particular, two HARQ schemes were examined, HARQ-CC and HARQ-IR. The outage performance of both HARQ schemes was investigated and closed-form analytical expressions were provided. Furthermore, the problem of minimizing the OP of the considered schemes under average and maximum optical power constraints was addressed. Power allocation schemes were developed, which distribute the optical power across the retransmission rounds and offer reduced power consumption as well as improve the throughput of the FSO systems. Simulation results validated the presented analysis and illustrated the improvement of the proposed HARQ schemes, in terms of both OP and throughput, compared to the fixed transmit power HARQ schemes. As a future study, FSO's performance can be improved by optimally adjusting the code rate of the HARQ-IR protocol across different retransmission rounds.

## ACKNOWLEDGEMENT

This work has received funding from the European Union's Horizon-JU- SNS-2022 research and innovation programme under grant agreement No. 101096456 (NANCY).

## APPENDIX

In the case of block-fading channel across all HARQ-CC rounds, the OP can be expanded using the [12, (9.303)] as (26), where  ${}_pF_q(\cdot; \cdot; \cdot)$  is the Generalized hypergeometric function. In high-SNR region we can see that  $V_R \rightarrow 0$ . Then, using the known property of Generalized hypergeometric function  $\lim_{z \rightarrow 0^+} {}_pF_q(a_1, \dots, a_p; b_1, \dots, b_q; z) = 1$ , we can write the asymptotic OP as the sum of three terms. The most dominant term is decided based on the values of  $\xi^2, \alpha, \beta$ . So, if  $\xi^2 < \min\{\alpha, \beta\}$ , then the OP can be approximated as

$$\mathbb{P}_{\text{out},j}^{\text{CC}} \approx \frac{\Gamma(\alpha - \xi^2) \Gamma(\beta - \xi^2)}{\Gamma(\alpha) \Gamma(\beta)} \left( \frac{V_R}{\sum_{i=1}^j P_i^2} \right)^{\xi^2/2} \tag{27}$$

if  $\xi^2 > \min\{\alpha, \beta\}$  the dominant term comes from the minimum of  $\alpha$  and  $\beta$  and is given by

$$\begin{aligned}
\mathbb{P}_{\text{out},j}^{\text{CC}} &\approx \frac{\Gamma(|\beta - \alpha|)}{(1 - \min\{\alpha, \beta\}/\xi^2) \Gamma(\min\{\alpha, \beta\} + 1) \Gamma(\max\{\alpha, \beta\})} \\
&\times \left( \frac{V_R}{\sum_{i=1}^j P_i^2} \right)^{\min\{\alpha, \beta\}/2}
\end{aligned}$$

## REFERENCES

- [1] L. Andrews, R. Philips, and C. Hopson, *Laser Beam Scintillation With Applications*, 01 2001.
- [2] Z. Shi, H. Ding, S. Ma, and K.-W. Tam, "Analysis of HARQ-IR over time-correlated Rayleigh fading channels," *IEEE Trans. Wireless Commun.*, vol. 14, no. 12, pp. 7096–7109, 2015.
- [3] H. D. Le and A. T. Pham, "Link-layer retransmission-based error-control protocols in FSO communications: A survey," *IEEE Commun. Surv. & Tut.*, vol. 24, no. 3, pp. 1602–1633, 2022.
- [4] S. M. Aghajanzadeh and M. Uysal, "Outage analysis of hybrid-ARQ protocols in coherent free-space optical communications," in *Proc. IEEE 22nd Int. Symp. Pers., Ind. and Mob. Radio Commun.*, 2011, pp. 1773–1777.
- [5] E. Zedini, A. Chelli, and M.-S. Alouini, "On the performance analysis of hybrid arq with incremental redundancy and with code combining over free-space optical channels with pointing errors," *IEEE Photonics J.*, vol. 6, no. 4, pp. 1–18, 2014.
- [6] G. Verma and A. Mathur, "Performance improvement of fso communication systems using hybrid-arq protocols," *Appl. Opt.*, vol. 60, 06 2021.
- [7] A. Touati, M. O. Hasna, and F. Touati, "HARQ performance over fso channels with atmospheric fading and pointing errors," in *Proc. 14th Int. Wireless Commun. Mob. Comp.*, 2018, pp. 158–163.
- [8] S. Das, H. Henniger, B. Eppler, C. I. Moore, W. Rabinovich, R. Sova, and D. Young, "Requirements and challenges for tactical free-space lasercomm," in *Proc. Mil. Commun. Conf. 2008*, 2008, pp. 1–10.
- [9] A. A. Farid and S. Hranilovic, "Outage capacity optimization for free-space optical links with pointing errors," *Journal of Lightwave Technology*, vol. 25, no. 7, pp. 1702–1710, 2007.
- [10] S. Arnon, J. R. Barry, G. K. Karagiannidis, R. Schober, and M. Uysal, *Advanced Optical Wireless Communication Systems*. Cambridge University Press, 2012.
- [11] H. G. Sandalidis, T. A. Tsiftsis, and G. K. Karagiannidis, "Optical wireless communications with heterodyne detection over turbulence channels with pointing errors," *J. Light. Technol.*, vol. 27, no. 20, pp. 4440–4445, 2009.
- [12] I. S. Gradshteyn and I. M. Ryzhik, *Table of Integrals, Series, and Products*, 6th ed. New York: Academic, 2000.
- [13] I. S. Ansari, F. Yilmaz, and M.-S. Alouini, "Performance analysis of FSO links over unified gamma-gamma turbulence channels," in *Proc. IEEE 81st Veh. Technol. Conf. (VTC Spring)*, 2015, pp. 1–5.
- [14] A. Chaaban, J.-M. Morvan, and M.-S. Alouini, "Free-space optical communications: Capacity bounds, approximations, and a new sphere-packing perspective," *IEEE Trans. Commun.*, vol. 64, no. 3, pp. 1176–1191, 2016.
- [15] M. Najafi, V. Jamali, P. D. Diamantoulakis, G. K. Karagiannidis, and R. Schober, "Non-orthogonal multiple access for FSO backhauling," in *Wireless Commun. Netw. Conf. (WCNC)*, 2018, pp. 1–6.
- [16] W. Su, S. Lee, D. A. Pados, and J. D. Matyjas, "Optimal power assignment for minimizing the average total transmission power in hybrid-ARQ Rayleigh fading links," *IEEE Trans. Commun.*, vol. 59, no. 7, pp. 1867–1877, 2011.
- [17] W. Rui and V. K. Lau, "Combined cross-layer design and harq for multiuser systems with outdated channel state information at transmitter (csit) in slow fading channels," *IEEE Trans. Wireless Commun.*, vol. 7, no. 7, pp. 2771–2777, 2008.